Conical Similarity of Shock/Boundary-Layer Interactions Generated by Swept and Unswept Fins

Gary S. Settles* and Frank K. Lu†
Pennsylvania State University, University Park, Pennsylvania

A parametric experimental investigation has been made of the class of three-dimensional shock wave/turbulent boundary-layer interactions generated by swept and unswept leading-edge fins. The fin sweepback angles were 0-65 deg at 5, 9, and 15 deg angles of attack. Two equilibrium two-dimensional turbulent boundary layers with a freestream Mach number of 2.95 and a Reynolds number of 6.3×10^7/m were used as incoming flow conditions. All of the resulting interactions were found to possess conical symmetry of the surface flow patterns and pressures outside of an initial inception zone. Further, these interactions were found to obey a simple conical similarity rule based on inviscid shock wave strength irrespective of fin sweepback or angle of attack. This is one of the first demonstrations of similarity among three-dimensional interactions produced by geometrically dissimilar shock generators.

Nomenclature

a	= exponent in Reynolds number scaling law
h	= fin height, cm
L_i	= length along inviscid shock wave trace on test surface for the inception of conical flow, cm
L_S	= length along inviscid shock wave trace from fin leading edge, cm
Lu_N	= upstream influence length normal to inviscid shock wave trace on test surface, cm
M_∞	= freestream Mach number
M_N	= $M_\infty \sin\beta_0$, component of freestream Mach number normal to inviscid shock wave trace on test surface
p	= surface static pressure, N/m^2
p_∞	= static pressure of the incoming freestream flow, N/m^2
$Re\delta$	= Reynolds number based on boundary-layer thickness
x,y,z	= Cartesian coordinate system (see Fig. 1)
x_S	= $x - z\cot\beta_0$, streamwise coordinate measured from inviscid shock wave trace on test surface
α	= fin angle of attack, deg
β_0	= inviscid shock wave angle on test surface measured from x axis, deg
β_A	= angle between conical flow attachment line and x axis, deg
β_{S1}	= angle between conical primary separation line and x axis, deg
β_{S2}	= angle between conical secondary separation line and x axis, deg
β_U	= angle between conical upstream influence line and x axis, deg
δ	= boundary-layer thickness, cm
δ_L	= local boundary-layer thickness just ahead of the upstream influence line, cm
ΔL_S	= displacement along the shock line of virtual conical origin from fin leading edge, cm
Δz	= spanwise displacement of virtual conical origin from fin leading edge, cm
λ	= fin leading-edge sweepback angle, deg
μ_∞	= freestream Mach angle, deg (= 19.8 deg at M = 2.95)

Introduction

THE interactions of shock waves and turbulent boundary layers constitute a classical problem of fluid dynamics that remains generally unsolved. These interactions, both two- and three-dimensional (2D and 3D), involve such a maze of flow regimes and peculiarities that no approximate analysis has shown much generality in their prediction. Further, numerical solutions of the nonlinear governing equations are currently possible only with limited methods of turbulence closure. This situation has led several investigators, including the present authors, to seek insight from experiments.

At least for 2D interactions, this experimental approach has been quite productive.[1-3] However, attempts to investigate 3D interactions have been fewer and less conclusive. Little overall understanding of the range of 3D interactions has been available until quite recently.

In an attempt to contribute to this poorly understood field, a series of parametric experiments has been performed in the past few years.[4-12] This paper presents recent results from that effort on the 3D interactions of turbulent boundary layers with shock waves generated by sharp fins.

Of many possible shock waves generators, the sharp fin has been used most often in 3D interaction experiments.[4,5,7,12-30] It produces a planar swept normal shock wave (also called a skewed or glancing oblique shock) with respect to a 2D boundary layer when its leading edge is normal to the plane of the boundary layer. This inviscid shock configuration, being planar, is perhaps the simplest 3D case available. However, the resulting 3D interaction of the shock with a viscous boundary layer is far from simple.

Even though this 3D interaction has been studied repeatedly, some investigators have failed to agree on basic considerations. For example, the literature[4,5,7,12-27] does not clarify whether the interaction is asymptotically cylindrical or conical in nature. Since sharp unbounded bodies naturally produce conical fields in supersonic flow, it appears likely to the present authors that earlier observations of quasicylindrical fin interactions were unintentionally contaminated by limited test channel or generator dimensions. In any case, there is still a need for a much improved understanding of fin-generated 3D shock/boundary-layer interactions.

The present study was made with that goal in mind. In particular, the parametric variation of a sharp fin leading-

Presented as Paper 83-1756 at the AIAA 16th Fluid and Plasma Dynamics Conference, Danvers, Mass., July 12-14, 1983; received Aug. 15, 1983; revision received Sept. 4, 1984. Copyright © American Institute of Aeronautics and Astronautics, Inc., 1984. All rights reserved.

*Associate Professor, Mechanical Engineering Department. Member AIAA.
†Graduate Student, Mechanical Engineering Department.

edge sweepback was included, since it had not been investigated in any known previous study. Such a sweepback produced nonplanar shock waves for comparison with the more familiar planar case. The specific goals of the work included the study of the shock shapes, the nature of the resulting interaction regimes, and the possibility of a unifying similarity principle for a wide range of interactions due to geometrically dissimilar fin-type shock generators. The general goal was primarily to gain insight into the flow phenomena and then to provide a data base for the validation of computational modeling attempts.

The reader is referred to Ref. 28 for the details of the experimental procedure and results. The present coverage is thus kept appropriately brief.

Experimental Procedures

Wind Tunnel and Models

The experiments were performed in the Princeton University supersonic blowdown wind tunnel. While some fin models were tested on the wind tunnel test section floor, the bulk of the data set was obtained using the flat-plate test geometry shown in Fig. 1.

A parametric set of 24 fin models was tested on this flat plate. These fins had leading-edge sweepback angles $\lambda = 0$, 10, 20, 30, 40, 50, 55, and 65 deg. Each of the fins was mounted perpendicular to the flat plate and was tested at angles of attack $\alpha = 5$, 9, and 15 deg.

Test Conditions

The tests were conducted at $M_\infty = 2.95$ with a stagnation temperature of 261 K$\pm$4%, a stagnation pressure of 0.689×10^6 N/m^2 $\pm$1%, and a nominal freestream Reynolds number of 6.3×10^7/m. (A few additional tests were performed at 18.7×10^7/m.) Fully developed, approximately adiabatic, zero-pressure-gradient turbulent boundary layers were developed on both the flat plate and the tunnel floor. These layers met the usual wall/wake law criterion for mean flow equilibrium. The boundary-layer thickness approaching the fin leading-edge position was 5 mm on the flat plate and 16 mm on the tunnel floor.

Techniques and Instrumentation

The present experiments consider mainly the mean "footprints" of fin-generated 3D interactions as revealed by surface flow visualization and static pressure measurements. The surface flow patterns were obtained by a special kerosene/lampblack/adhesive tape technique.[9] Surface pressures were read from several streamwise rows of taps connected to a computer-controlled Scanivalve bank. Extensive comparisons of these results have shown that they give equivalent indications of upstream influence in shock/boundary-layer interactions.[7-9]

In addition to these measurements, flowfield shadowgraphy was used to determine the shock wave shapes and angles (as described below). A localized vapor-screen technique was also used to visualize the 3D flow separation.

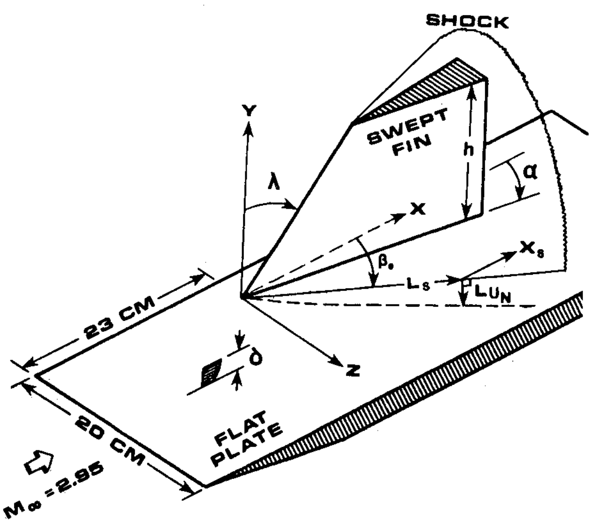

Fig. 1 Flat plate and swept fin test geometry.

Results and Discussion

Vapor Screen Flow Visualization

There has been a technical controversy over the definition of 3D flow separation,[31] especially when it is evidenced only by surface-streak patterns. Many investigators accept the view of Maskell[32] that an envelope or asymptotic convergence of surface-streak lines defines a 3D separation line at which the boundary layer leaves the surface to which it was formerly attached. Nonetheless, the authors sought an independent means to confirm or deny this hypothesis in the context of the present study.

A suitable means to that end is the localized vapor-screen flow visualization technique.[9] A thin stream of acetone was injected into the flow through a pressure tap near the junction of the fin leading edge and flat plate. For fins at $\alpha = 5$ deg (unseparated by any definition at Mach 2.95), the acetone merely flowed downstream along the fin/plate junction. However, at $\alpha = 9$ and 15 deg, the acetone flowed outward along the surface-streak convergence line and was partially atomized by the flow, forming a continuous aerosol "sheet" that left the plate surface. This phenomenon was visualized using a 2 mm thick plane of light expanded from a 2 W argon-ion laser beam. The results were photographed and videotaped while the laser light sheet was scanned across the flow.

These visualization results gave a clear picture of 3D flow separation, as demonstrated in Fig. 2. Here, the light sheet is vertical and roughly normal to the shock wave generated by the $\alpha = 15$ deg, $\lambda = 0$ deg fin, while the camera view is roughly normal to the light sheet. The acetone fog marking the separated shear layer is seen to leave the surface-streak convergence line S1, reach a significant height above the test surface, and then return to the surface at the streak divergence line A.

Unfortunately, no clear visualization of the flowfield immediately above the "secondary separation" line S2 could be obtained with this technique. Thus, line S2 is referred to as secondary separation on the basis of surface/streakline convergence alone. Note that, with reference to previous studies in which such a line was observed[27,33] and to topological considerations,[34] the line S2 in all of the present flows appears to represent a near-incipient condition of secondary flow separation.

Inviscid Shock Wave Shape

The "inviscid shock wave" is defined here as the shock wave that would exist in Fig. 1 if no viscous boundary layer and thus no interaction were present. However, even with this simplification, the shock shape is only known a priori

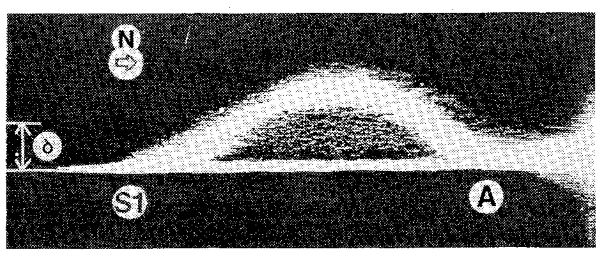

Fig. 2 Local vapor-screen visualization of 3D boundary-layer separation and reattachment.

for unswept fins ($\lambda = 0$ deg), where it is planar and calculable from oblique shock theory. Otherwise, for $\lambda > 0$ deg but less than the detachment value, the shock forms a conical envelope exactly like that about a planar delta wing at angle of attack,[35] with the flat plate of Fig. 1 acting as a streamwise plane of symmetry through the wing apex.

For present purposes, it is primarily necessary to know the intersection or "trace" of the inviscid shock on the flat plate. This trace is the best available reference position from which to measure the extent of the shock/boundary-layer interaction.[11] Observe that continuity requires the inviscid shock to be locally normal to the flat plate in Fig. 1 (a matter of considerable importance in the later discussion). Also observe that, according to conical flow theory, the inviscid shock trace on the plate must be a straight line through the coordinate origin in Fig. 1. The definition of this trace thus requires only that a single angle, β_0, be specified.

This angle can be estimated by an approximate method due to Roe,[36] calculated using a shock-fitting numerical solution of the Euler equations, or determined directly from experiments. The latter method was chosen as the most accurate and straightforward for present purposes. Flat delta wings duplicating the (α,λ) parameters of the present fin shock generators were mounted on the wind tunnel centerline and observed by shadowgraph visualization. As illustrated in Fig. 3, this allowed the direct measurement of β_0 from shadowgrams.

Further, for delta wings with shocks attached to the leading edges, serrations on these leading edges generated Mach waves on the conical shock envelope from which the shock shape could be determined. An example of this is given in Fig. 4. The resulting shock shapes and β_0 values were in general agreement with calculated values using Roe's method,[36] although the latter tended to underestimate the measured values of β_0 somewhat.

A summary of the shadowgram results for $\beta_0(\alpha,\lambda)$ is plotted in Fig. 5. Clearly, β_0 is a strong function of α but a mild function of λ. These data are prerequisites for the following analysis of fin-generated conical shock/boundary-layer interactions.

Conical Interaction Symmetry

Figure 6a presents an example of a kerosene/lampblack/adhesive tape surface flow visualization pattern show-

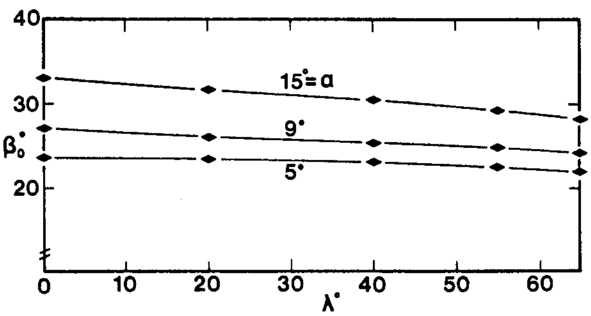

Fig. 5 Measured and interpolated shock angles β_0 for $M_\infty = 2.95$.

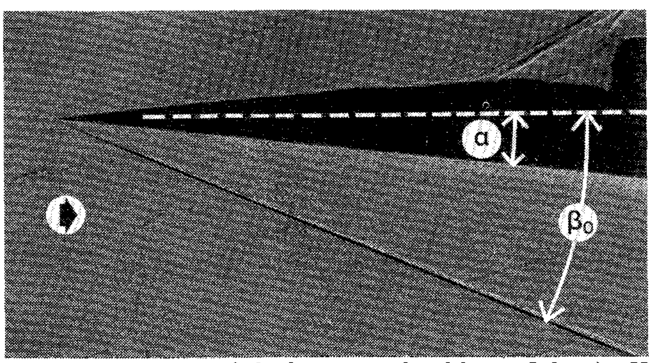

Fig. 3 Shadowgram of shock wave produced by $\alpha = 5$ deg, $\lambda = 55$ deg delta wing.

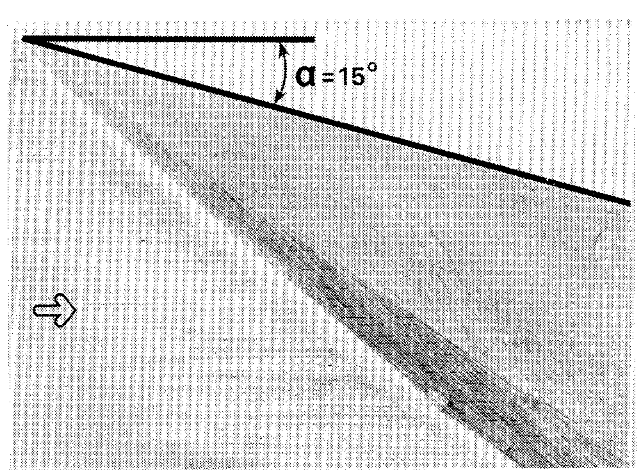

Fig. 6a Example of kerosene/lampblack/adhesive tape surface-streak pattern for $\alpha = 15$ deg, $\lambda = 0$ deg fin interaction on flat plate.

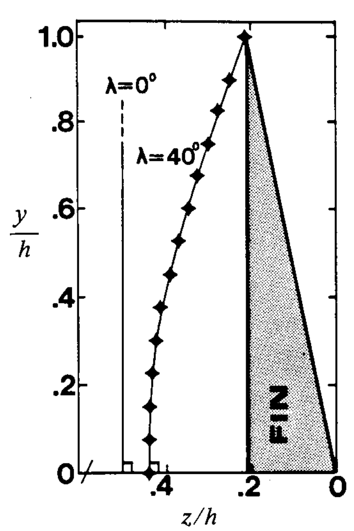

Fig. 4 Shock wave shapes for $\lambda = 40$ deg delta wing and corresponding unswept wing at $\alpha = 15$ deg (looking upstream).

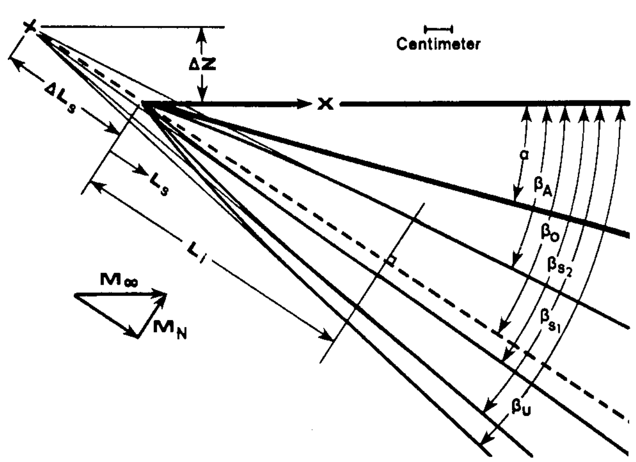

Fig. 6b Corresponding diagram of interaction footprint features and notation.

ing the "footprint" of the $\alpha = 15$ deg, $\lambda = 0$ deg fin interaction. Figure 6 is a geometrically similar diagram of this footprint showing the framework and defining the parameters used in the present analysis of such patterns. Distances are represented either by the streamwise x coordinate or by the L_S coordinate. All angles are measured from the x axis.

For every (α,λ) combination tested, the interaction footprint was observed to begin at the flat-plate/fin leading-edge junction with a curved, nonconical "inception zone."[11,25] Beyond this zone, i.e., for $L_S > L_i$, *conical interaction symmetry* was observed.[11,12,24,25,27-30,37]

By definition, all surface features in the conical region are bounded by rays from a common origin. However, due to the inception zone this origin does not coincide with the plate/leading-edge junction. It is instead a virtual origin that is displaced by a distance ΔL_S along the inviscid shock line, as shown in Fig. 6b.

Four features of the surface streak pattern of Fig. 6a are indicated in Fig. 6b. These features run asymptotically into straight lines through the virtual conical origin at angles $\beta_{\langle\rangle}$ with the x axis. They are the upstream influence line β_U, the primary separation line at β_{S1}, the secondary separation line at β_{S2}, and the primary reattachment line at β_A. Also shown for reference is the inviscid shock trace (dashed line) at β_0, although it does not constitute a surface pattern feature.

Obviously, some of these features are present in the surface streak patterns only when the shock is strong enough to cause 3D separation of the boundary layer. Also, note that the fin/plate junction at angle α in Fig. 6b does not lie along a ray from the conical virtual origin and thus is not a conical feature of the interaction. (Indeed, a close examination of the surface patterns reveals flow across this junction.)

Asymptotically conical symmetry was observed for all the present fin interactions in both surface-streak patterns and surface pressure distributions. This is shown by the example of the $\alpha = 15$ deg, $\lambda = 55$ deg fin interaction in Fig. 7. The normalized surface pressure p/p_∞ is plotted against $x_S/(z+\Delta z)$ and is shown to be invariant with spanwise distance in these coordinates.‡ Thus, the fact that the streamwise interaction scale is proportional to the spanwise distance from the virtual origin in Fig. 7 and in the other pressure distributions (not shown) lends further support to conical interaction symmetry.

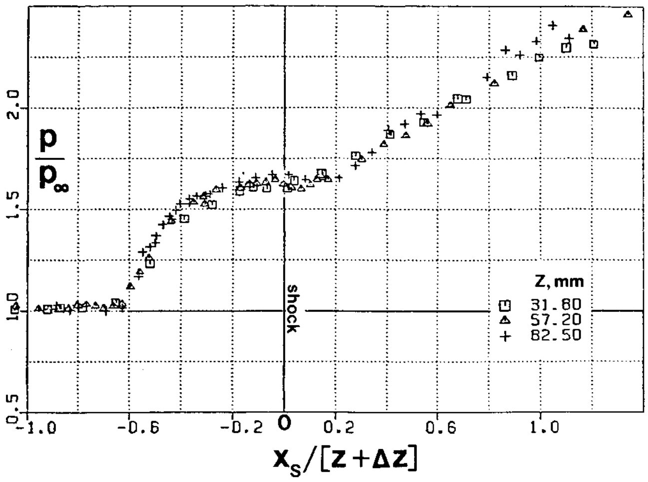

Fig. 7 Streamwise surface pressure distributions for $\alpha = 15$ deg, $\lambda = 55$ deg swept fin interaction, scaled by spanwise distance from virtual conical origin.

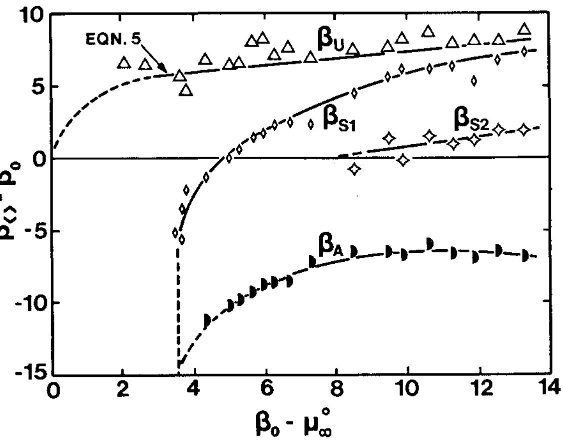

Fig. 8 Angular response of interaction features vs shock wave strength, demonstrating results of parametric variation of α and λ.

Conical Interaction Similarity

Having observed conical symmetry for both swept and unswept fin interactions raises the possibility of similarity among them. In other words, are swept and unswept interactions fundamentally different or are they similar in some appropriate framework? This question is addressed by the results shown in Fig. 8.

The ordinate of Fig. 8 represents an "interaction response function," i.e., the difference between any of the conical surface feature angles $\beta_{\langle\rangle}$ and the shock angle β_0. The abscissa of Fig. 8 represents the shock wave strength at the test surface by the quantity $\beta_0 - \mu_\infty$. The results show clearly that the interaction features are functions of $\beta_0 - \mu_\infty$ (or of β_0 alone, since $\mu_\infty = \text{const}$) irrespective of the fin geometry parameters α and λ.

This discovery amounts to a straightforward conical similarity of fin-generated 3D interactions. The fin geometry and overall shock shape appear not to influence the shock/boundary-layer interaction other than in specifying the inviscid shock angle at the test surface. The authors believe this to be a unique demonstration of similarity among interactions produced by geometrically dissimilar shock generators.

The following physical explanation is put forth for this phenomenon. Recall that continuity requires the inviscid shock to be normal to the test surface in all cases. If the inviscid shock configuration in the immediate vicinity of the boundary layer it interacts with is of primary importance in specifying the interaction, then planar and weakly curved shocks of equal β_0 will produce equivalent interactions. The overall shock shape will be immaterial in this case§ and the conical similarity shown in Fig. 8 will then be a direct result.

This explanation of conical similarity assumes that the 3D interaction problem can be simplified to local rather than global flow conditions. The general validity of this assumption for other than fin-generated interactions with both separation and reattachment in the plane of the incoming boundary layer is a subject of ongoing study.[12]

A second assumption is also implicit in the above physical explanation. While the character of the flows observed here

‡The use of (x,z) rather than shock-based normal and tangential coordinates here is admittedly clumsy, but necessary since the surface pressure tap rows were all parallel to the x axis. Note further that the Δz value used in constructing Fig. 7 was obtained from the corresponding surface-streak pattern, as was the case for all the present experiments.[28]

§Recent research[12] has shown that, for interactions due to different shock generators where the inviscid shock wave radius of curvature is comparable to the boundary-layer thickness, the shock shape must also be taken into account along with the angle β_0. For all the present fin interactions, however, the shock radius was at least an order of magnitude larger than the boundary-layer thickness.

is clearly the result of an interaction of viscous and inviscid phenomena, the latter appear to play a predominant role in specifying the overall flow symmetry and scaling parameters.

A further test of conical similarity should be made by varying M_∞. While β_0 alone is sufficient to specify the shock strength with M_∞ fixed, note that $M_N = M_\infty \sin\beta_0$ is required for that purpose when M_∞ varies. Whether or not conical similarity based on M_N holds in general should be one subject of future study.

Finally, before leaving Fig. 8, there are several additional observations of value:

1) Incipient primary flow separation occurs at $\beta_0 - \mu_\infty = 3.5$ deg, corresponding closely to Korkegi's[38] simple criterion.

2) Incipient "secondary separation" occurs at $\beta_0 - \mu_\infty = 8$ deg, corresponding closely to Zheltovodov's[24] modification of Korkegi's criterion.

3) Stanbrook's[14] definition of incipient 3D separation as the condition where the surface-streak angle first equals the shock angle is not supported by Fig. 8. In fact, incipient separation occurs when the streak angle is about 6 deg less than the shock angle in the present experiments.

4) The angular difference between the upstream influence and primary separation lines is a significant fraction of the total interaction footprint near incipient separation, but shrinks toward a negligible value as the shock strength is increased.

5) Finally, note that the region of vanishingly weak shock strength in Fig. 8 $[0 \leq (\beta_0 - \mu_\infty) \leq 4$ deg$]$ apparently involves a rapid nonlinear growth of upstream influence. This was first noted by Dolling,[7] who also pointed out that accurate measurements in this weak shock region are prohibitively difficult.

Reynolds Number and Shock Strength Similarity

Settles[8] has previously formulated a scaling law for Reynolds number effects on 3D interactions that succeeded in correlating the results of both swept compression corner[8,39] and unswept fin[7,29,30] interactions. Dolling[7] extended this scaling law to include variable shock strength in unswept fin interactions by way of the normal Mach number M_N. In coordinates normal and tangential to the inviscid shock wave, this scaling law can be written for the upstream influence as

$$(Lu_N/\delta_L)(Re\delta_L^a/M_N) = f[(L_S/\delta_L)Re\delta_L^a] \tag{1}$$

where a has an empirical value of about ⅓ when $M_\infty = 2.95$.

The applicability of Eq. (1) to both swept and unswept fin interactions has been tested by plotting the present upstream influence data in terms of the above coordinates in Fig. 9. Included in this figure are 41 upstream influence lines embodying parametric variations of α, λ, δ_L, and $Re\delta_L$. The result clearly indicates that Eq. (1) is applicable to both swept and unswept fin interactions within the present ranges of parameters.

One observation drawn from Fig. 9 is that the simple normalization of Lu_N by M_N effectively correlates variations in shock strength due to both α and λ variations of the fin geometry. This result is thus an additional confirmation of the conical similarity principle, since

$$M_N = M_N(M_\infty, \alpha, \lambda) = M_\infty \sin\beta_0(\alpha, \lambda) \tag{2}$$

As stated earlier, a more rigorous test would be possible if data were available at other values of M_∞. Simple normalization by M_N could be an oversimplification with a limited range of validity, although it is certainly effective for the present limited range of fin interactions at $M_\infty \simeq 3$ as supported by Fig. 9. However, recent research[12] has shown that related interactions, produced by swept compression corners at the same M_∞, scale according to M_N^2 rather than M_N. This raises questions that cannot be answered at present, other than to point out that M_N^2 scaling has the physical justification of being directly related to the shock wave strength via the pressure ratio, while simple M_N scaling apparently lacks any such justification.

Returning to Fig. 9, note that the length of the nonconical interaction inception zone L_i is given approximately by

$$(L_i/\delta_L)Re\delta_L^{1/3} \sim 1600 \quad (M_\infty = 2.95) \tag{3}$$

This number is difficult to determine accurately due to the asymptotic joining of the inception and conical zones. Further, recent research[40] covering larger values of α indicates a tendency for L_i to grow as α increases.

One consequence of Eq. (3) is that the inception zone for the case of an extremely thin boundary layer and high Reynolds number may have a negligible dimensional length, as found by Zubin and Ostapenko.[25] On the other hand, the opposite conditions can expand the length of the inception zone beyond the size of the test facility itself (as seen in the results of Token,[18] even though his experiments were carried out on a massive dimensional scale).

Clearly, the inception zone, which is the only dimensional region in an otherwise nondimensional conical interaction, can itself be understood only in nondimensional terms. A rational hypothesis for its existence[41] is based on the comparable scales of the incoming boundary layer and the initial interaction region near the fin leading-edge/flat-plate junction, hence the $Re\delta_L$ dependence in Eq. (3).

Outside the inception zone the flow has been shown to be conical, so length dimensions and Reynolds number no longer have any relevance to the scaling. In this case, Eq. (1) may be rewritten as

$$Lu_N/(L_S + \Delta L_S) = \tan(\beta_U - \beta_0) = c_l M_N \quad (L_S \geq L_i) \tag{4}$$

where the coordinate origin has been shifted to the virtual conical origin and the constant $c_l \simeq 0.09$ is simply the slope

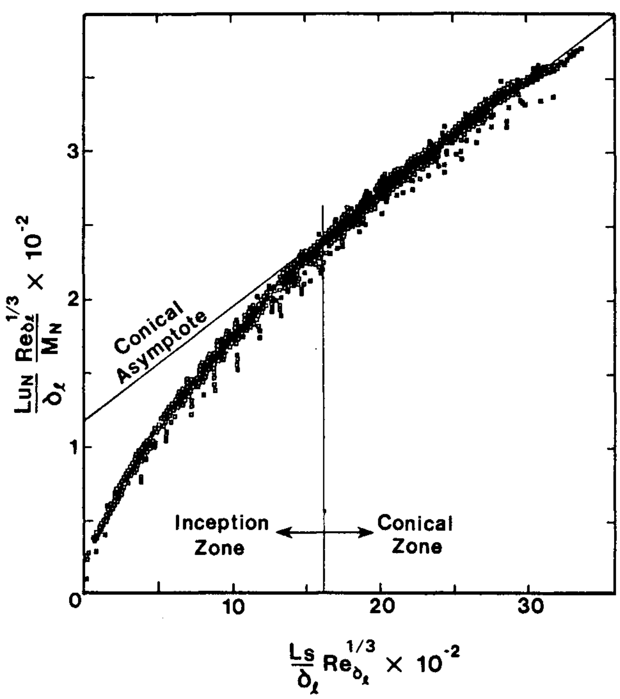

Fig. 9 Scaling of upstream influence lines across the present (α, λ) range in nondimensional form.

of the conical asymptote in Fig. 9. Expanding M_N,

$$\tan(\beta_U - \beta_0) = c_1 M_\infty \sin\beta_0 = c_2 \sin\beta_0 \quad (M_\infty = 2.95)$$

$$(\beta_U - \beta_0) = \arctan(0.26\sin\beta_0) \qquad (5)$$

where $c_2 = c_1 M_\infty = 0.26$. Equation (5) is, in fact, the straight line through the β_U data shown in Fig. 8. Thus, at least for the upstream influence, the normal Mach number scaling of Eq. (1) and the principle of conical similarity are equivalent over the range of the present experiments.

Conclusion

A parametric experimental study of swept-fin-induced three-dimensional shock wave/turbulent boundary-layer interactions has been carried out at $M_\infty = 2.95$. Included in the study were 2 incoming boundary layers, 2 values of Reynolds number, and 24 values of fin sweepback and angle of attack. The results consisted of surface and flowfield visualization data and surface pressure measurements. A scaling framework was developed for the analysis of these results. The major conclusions drawn from this analysis are:

1) Three-dimensional boundary-layer separation was clearly observed at lines of streak convergence on the interaction test surface.

2) Asymptotically conical shock/boundary-layer interactions were produced under all the present test conditions.

3) These interactions were found to obey a conical similarity principle based on local shock wave strength in the vicinity of the boundary layer irrespective of fin sweepback or angle of attack.

4) Scaling laws for Reynolds number and normal Mach number effects, developed in earlier studies, were found to apply equally well to the present swept and unswept fin interactions.

Acknowledgments

This work was supported by NASA Grant NAG2-109 monitored by Dr. C. C. Horstman and by AFOSR Contract F49620-81-K-0018 monitored by Dr. J. D. Wilson. The work was performed while both authors were with the Gas Dynamics Laboratory, Princeton University. The authors acknowledge helpful discussions with Profs. S. M. Bogdonoff and D. S. Dolling and Mr. R. L. Kimmel.

References

[1]Green, J. E., "Interaction Between Shock Waves and Boundary Layers," *Progress in Aerospace Sciences*, Vol. 11, Pergamon Press, New York, 1970, pp. 235-340.

[2]Hankey, W. L. Jr. and Holden, M. S., "Two-Dimensional Shock-Wave Boundary-Layer Interactions in High Speed Flows," AGARDograph No. 203, 1975.

[3]Stanewsky, E., "Shock-Boundary Layer Interaction in Transonic and Supersonic Flow," von Kármán Institute, Belgium, Rept. VKI-LS-59, 1973.

[4]Oskam, B., Vas, I. E., and Bogdonoff, S. M., "Mach 3 Oblique Shock Wave/Turbulent Boundary Layer Interactions in Three Dimensions," AIAA Paper 76-336, July 1976.

[5]Dolling, D. S., "Comparison of Sharp and Blunt Fin-Induced Shock Wave/Turbulent Boundary-Layer Interaction," *AIAA Journal*, Vol. 20, Oct. 1982, pp. 1385-1391.

[6]Settles, G. S., Perkins, J. J., and Bogdonoff, S. M., "Investigation of Three-Dimensional Shock/Boundary Layer Interactions at Swept Compression Corners," *AIAA Journal*, Vol. 18, July 1980, pp. 779-785.

[7]Dolling, D. S., "Upstream Influence in Sharp Fin-Induced Shock Wave Turbulent Boundary-Layer Interaction," *AIAA Journal*, Vol. 21, Jan. 1983, pp. 143-145.

[8]Settles, G. S. and Bogdonoff, S. M., "Scaling of Two- and Three-Dimensional Shock/Turbulent Boundary Layer Interactions at Compression Corners," *AIAA Journal*, Vol. 20, June 1982, pp. 782-789.

[9]Settles, G. S. and Teng, H.-Y., "Flow Visualization Methods for Separated Three-Dimensional Shock Wave/Turbulent Boundary Layer Interactions," *AIAA Journal*, Vol. 21, March 1983, pp. 390-397.

[10]Settles, G. S. and Teng, H.-Y., "A Test of the Independence Principle in Swept Cylindrical Shock Wave/Turbulent Boundary Layer Interactions," Paper presented at 2nd Asian Congress of Fluid Mechanics, Beijing, China, Oct. 25-29, 1983.

[11]Settles, G. S. and Teng, H.-Y., "Cylindrical and Conical Flow Regimes of Three-Dimensional Shock/Boundary-Layer Interactions," *AIAA Journal*, Vol. 22, Feb. 1984, pp. 194-200.

[12]Settles, G. S. and Kimmel, R. L., "Similarity Conditions for Conical Shock Wave/Turbulent Boundary Layer Interactions," AIAA Paper 84-1557, June 1984.

[13]Gadd, G. E., "Interactions Between Shock Waves and Boundary Layers," *Proceedings of the Symposium on Boundary Layer Research*, edited by H. Gortler, Springer Verlag, Freiburg, FRG, 1957, pp. 239-255.

[14]Stanbrook, A., "An Experimental Study of the Glancing Interaction Between a Shock Wave and a Boundary Layer," British Aeronautical Research Council, CP-555, July 1960.

[15]McCabe, A., "A Study of Three-Dimensional Interactions Between Shock Waves and Turbulent Boundary Layers," Ph.D. Thesis, University of Manchester, England, Oct. 1963.

[16]Lowrie, B. W., "Cross-Flows Produced by the Interaction of a Swept Shock Wave with a Turbulent Boundary Layer," Ph.D. Thesis, Cambridge University, England, Dec. 1965.

[17]Goldberg, T. J., "Three-Dimensional Separation for Interaction of Shock Waves with Turbulent Boundary Layers," *AIAA Journal*, Vol. 11, Nov. 1973, pp. 1573-1575.

[18]Token, K. H., "Heat Transfer due to Shock Wave Turbulent Boundary Layer Interactions on High Speed Weapon Systems," AFFDL-TR-74-77, April 1974.

[19]Neumann, R. D. and Token, K. H., "Prediction of Surface Phenomena Induced by Three-Dimensional Interactions on Planar Turbulent Boundary Layers," Paper 74-058 presented at 25th IAF Congress, Amsterdam, 1974.

[20]Peake, D. J., "The Three-Dimensional Interaction of a Swept Shock Wave with a Turbulent Boundary Layer and the Effects of Air Injection on Separation," Ph.D. Thesis, Carleton University, Ottawa, Canada, 1975.

[21]Law, C. H., "Three-Dimensional Shock Wave/Turbulent Boundary Layer Interactions at Mach 6," ARL-TR-75-0191, June 1975.

[22]Cousteix, J. and Houdeville, R., "Epaississement et Separation d'une Couche Limite Turbulent Soumise en Interaction avec un Choc Oblique," *La Recherche Aerospatiale*, Jan.-Feb. 1976, pp. 1-11.

[23]Hayes, J. R., "Prediction Techniques for the Characteristics of Fin Generated Three-Dimensional Shock Wave Turbulent Boundary Layer Interactions," AFFDL-TR-77-10, May 1977.

[24]Zheltovodov, A. A., "Properties of Two- and Three-Dimensional Separation Flows at Supersonic Velocities," *Izvestiya Akademii Nauk SSSR, Mekhanika Zhidkosti i Gaza*, No. 3, May-June 1979, pp. 42-50.

[25]Zubin, M. A. and Ostapenko, N. A., "Structure of Flow in the Separation Region Resulting from Interaction of a Normal Shock Wave with a Boundary Layer in a Corner," *Izvestiya Akademii Nauk SSSR, Mekhanika Zhidkosti i Gaza*, No. 3, May-June 1979, pp. 51-58.

[26]Kubota, H. and Stollery, J. L., "An Experimental Study of the Interaction Between a Glancing Shock Wave and a Turbulent Boundary Layer," *Journal of Fluid Mechanics*, Vol. 116, 1982, pp. 431-458.

[27]Zheltovodov, A. A., "Regimes and Properties of Three-Dimensional Separation Flows Initiated by Skewed Compression Shocks," *Zhurnal Prikladnoi Mekhaniki i Tekhnicheskoi Fiziki*, No. 3, May-June 1982, pp. 116-123.

[28]Lu, F. K., "An Experimental Study of Three-Dimensional Shock Wave/Boundary Layer Interactions Generated by Sharp Fins," M.S.E. Thesis 1584-T, Mechanical & Aerospace Engineering Dept., Princeton University, Princeton, N.J., Nov. 1982.

[29]Degrez, G. and Ginoux, J. J., "Three-Dimensional Skewed Shock Wave Laminar Boundary Layer Interaction at Mach 2.25," AIAA Paper 83-1755, July 1983.

[30]McClure, W. B. and Dolling, D. S., "Flowfield Scaling in Sharp Fin-Induced Shock Wave Turbulent Boundary Layer Interaction," AIAA Paper 83-1754, July 1983.

[31]Peake, D. J. and Rainbird, W. J., "Technical Evaluation Report on the Fluid Dynamics Panel Symposium on Flow Separation," AGARD AR-98, Oct. 1976.

[32]Maskell, E. C., "Flow Separation in Three Dimensions," British Royal Aeronautical Establishment, Rept. 2565, Nov. 1955.

[33]Korkegi, R. H., "On the Structure of Three-Dimensional Shock-Induced Separated Flow Regions," *AIAA Journal*, Vol. 14, May 1976, pp. 597-600.

[34]Peake, D. J. and Tobak, M., "Three-Dimensional Interactions and Vortical Flows with Emphasis on High Speeds," NASA TM 81169, March 1980.

[35]Fowell, L. R., "Exact and Approximate Solutions for the Supersonic Delta Wing," *Journal of the Aeronautical Sciences*, Vol. 22, Aug. 1956, pp. 709-720.

[36]Roe, P. L., "A Simple Treatment of the Attached Shock Layer on a Delta Wing," British Royal Aeronautical Establishment, TR 70246, Dec. 1970.

[37]Avduyevskii, V. S. and Gretsov, V. K., "Investigation of the Three-Dimensional Separation Flow Around Semicones on a Flat Plate," *Izvestiya Akademii Nauk SSSR, Mekhanika Zhidkosti i Gaza*, No. 6, Nov.-Dec. 1970, pp. 112-115.

[38]Korkegi, R. H., "A Simple Correlation for Incipient Turbulent Boundary-Layer Separation due to a Skewed Shock Wave," *AIAA Journal*, Vol. 11, Nov. 1973, pp. 1578-1579.

[39]Settles, G. S., Horstman, C. C., and McKenzie, T. M., "Flowfield Scaling of a Swept Compression Corner Interaction—A Comparison of Experiment and Computation," AIAA Paper 84-0096, Jan. 1984.

[40]Goodwin, S. P., "An Exploratory Investigation of Sharp Fin-Induced Shock Wave/Turbulent Boundary-Layer Interactions at High Shock Strengths," M.S.E. Thesis 1687-T, Mechanical and Aerospace Engineering Dept., Princeton University, Princeton, N.J., Nov. 1984.

[41]Settles, G. S., "On the Inception Lengths of Swept Shock Wave/Turbulent Boundary-Layer Interactions," paper to be presented at IUTAM Symposium on Turbulent Shear Layer/Shock Wave Interactions, Paris, Sept. 1985.

From the AIAA Progress in Astronautics and Aeronautics Series...

FUNDAMENTALS OF SOLID-PROPELLANT COMBUSTION – v.90

Edited by Kenneth K. Kuo, The Pennsylvania State University
Martin Summerfield, Princeton Combustion Research Laboratories, Inc.

In this volume distinguished researchers treat the diverse technical disciplines of solid-propellant combustion in fifteen chapters. Each chapter presents a survey of previous work, detailed theoretical formulations and experimental methods, and experimental and theoretical results, and then interprets technological gaps and research directions. The chapters cover rocket propellants and combustion characteristics; chemistry ignition and combustion of ammonium perchlorate-based propellants; thermal behavior of RDX and HMX; chemistry of nitrate ester and nitramine propellants; solid-propellant ignition theories and experiments; flame spreading and overall ignition transient; steady-state burning of homogeneous propellants and steady-state burning of composite propellants under zero cross-flow situations; experimental observations of combustion instability; theoretical analysis of combustion instability and smokeless propellants.

For years to come, this authoritative and compendious work will be an indispensable tool for combustion scientists, chemists, and chemical engineers concerned with modern propellants, as well as for applied physicists. Its thorough coverage provides necessary background for advanced students.

Published in 1984, 891 pp., 6×9 illus. (some color plates), $60 Mem., $85 List; ISBN 0-915928-84-1

TO ORDER WRITE: Publications Order Dept., AIAA, 1633 Broadway, New York, N.Y. 10019